




# Syk Activation in Circulating and Tissue Innate Immune Cells in Antineutrophil Cytoplasmic Antibody–Associated Vasculitis

Maria Predecki,<sup>1</sup>  Kavita Gulati,<sup>1</sup>  Noelle Pisacano,<sup>2</sup> Damilola Pinheiro,<sup>3</sup> Tejal Bhatt,<sup>3</sup> Marie-Anne Mawhin,<sup>3</sup> Frederic Toulza,<sup>3</sup> Esteban S. Masuda,<sup>4</sup> Andrew Cowburn,<sup>2</sup> Katharine M. Lodge,<sup>2</sup> Frederick W. K. Tam,<sup>1</sup> Candice Roufousse,<sup>3</sup> Charles D. Pusey,<sup>1</sup> and Stephen P. McAdoo<sup>1</sup> 

**Objective.** Syk is a cytoplasmic protein tyrosine kinase that plays a role in signaling via B cell and Fc receptors (FcR). FcR engagement and signaling via Syk is thought to be important in antineutrophil cytoplasm antibody (ANCA) IgG–mediated neutrophil activation. This study was undertaken to investigate the role of Syk in ANCA-induced myeloid cell activation and vasculitis pathogenesis.

**Methods.** Phosphorylation of Syk in myeloid cells from healthy controls and ANCA-associated vasculitis (AAV) patients was analyzed using flow cytometry. The effect of Syk inhibition on myeloperoxidase (MPO)–ANCA IgG activation of cells was investigated using functional assays (interleukin-8 and reactive oxygen species production) and targeted gene analysis with NanoString. Total and phosphorylated Syk at sites of tissue inflammation in patients with AAV was assessed using immunohistochemistry and RNAscope in situ hybridization.

**Results.** We identified increased phosphorylated Syk at critical activatory tyrosine residues in blood neutrophils and monocytes from patients with active AAV compared to patients with disease in remission or healthy controls. Syk was phosphorylated in vitro following MPO–ANCA IgG stimulation, and Syk inhibition was able to prevent ANCA-mediated cellular responses. Using targeted gene expression analysis, we identified up-regulation of FcR- and Syk-dependent signaling pathways following MPO–ANCA IgG stimulation. Finally, we showed that Syk is expressed and phosphorylated in tissue leukocytes at sites of organ inflammation in AAV.

**Conclusion.** These findings indicate that Syk plays a critical role in MPO–ANCA IgG–induced myeloid cell responses and that Syk is activated in circulating immune cells and tissue immune cells in AAV; therefore, Syk inhibition may be a potential therapeutic option.

## INTRODUCTION

Syk is a cytoplasmic protein tyrosine kinase that plays a role in signaling via classical immunoreceptors bearing immunoreceptor tyrosine–based activation motifs (ITAM), including B cell and activatory Fc receptors (FcR). As such, it is highly expressed in myeloid cells, where it is known to mediate important

FcR-dependent inflammatory responses (1–3). The Syk protein has a multidomain structure, consisting of 2 SH2 domains and a C-terminal kinase domain (4). In the inactivated state, the C-terminal kinase domain is retained within a folded or “closed” tertiary structure. Following cell surface immunoreceptor ligation, ITAM serve as binding sites for Syk SH2 domains, resulting in auto- and transphosphorylation of Syk tyrosine residues,

Presented in abstract form at the 19th International Vasculitis and ANCA Workshop in Philadelphia, PA, in April 2019 (<https://doi.org/10.1093/rheumatology/kez061.027>).

Supported by the NIHR Imperial Biomedical Research Centre. Dr. Predecki's work was supported by the Academy of Medical Sciences (grant SGL023/1071) and by an NIHR Clinical Lectureship. Dr. Tam's work was supported by the Ken and Mary Minton Chair of Renal Medicine. Dr. McAdoo's work was supported by Vasculitis UK and by an Imperial College Wellcome Trust ISSF Fellowship.

<sup>1</sup>Maria Predecki, MBBS, PhD, Kavita Gulati, MBCh, BAO, Frederick W.K. Tam, PhD, MBChir, Charles D. Pusey, DSc, FMedSci, Stephen P. McAdoo, MBBS, PhD: Department of Immunology and Inflammation, Centre for Inflammatory Disease, Imperial College London, Hammersmith Campus, and Imperial College Renal and Transplant Centre, Imperial College Healthcare NHS Trust,

Hammersmith Hospital, London, UK; <sup>2</sup>Noelle Pisacano, MSc, Andrew Cowburn, PhD, Katharine M. Lodge, PhD, MBChir: National Heart and Lung Institute, Imperial College, London, UK; <sup>3</sup>Damilola Pinheiro, PhD, Tejal Bhatt, MSc, Marie-Anne Mawhin, PhD, Frederic Toulza, PhD, Candice Roufousse, MD, PhD: Department of Immunology and Inflammation, Centre for Inflammatory Disease, Imperial College London, Hammersmith Campus, London, UK; <sup>4</sup>Esteban S. Masuda, PhD: Rigel Pharmaceuticals, South San Francisco, California.

Author disclosures are available at <https://onlinelibrary.wiley.com/action/downloadSupplement?doi=10.1002%2Fart.42321&file=art42321-sup-0001-Disclosureform.pdf>.

Address correspondence via email to Predecki, MBBS, PhD, at [m.predecki@imperial.ac.uk](mailto:m.predecki@imperial.ac.uk).

Submitted for publication November 23, 2021; accepted in revised form July 26, 2022.

conformational changes that release the enzymatically active kinase domain, and initiation of downstream signaling (5–7). Thus, Syk activity relies upon its phosphorylation status at multiple tyrosine residues, and phosphorylation at Y<sup>352</sup> and Y<sup>348</sup> has been shown to be essential for downstream Syk signaling (8–10).

In antineutrophil cytoplasm antibody (ANCA)-associated vasculitis (AAV), ANCA may contribute to disease pathogenesis via binding to their cognate antigens (proteinase 3 and myeloperoxidase [MPO]) on the surface of primed neutrophils and monocytes, resulting in cell activation and subsequent vascular injury (11,12). Both FcR engagement and autoantigen-specific binding via F(ab) are thought to be important in ANCA-mediated cell activation, with evidence for signaling through the low-affinity Fcγ receptor (FcγR) FcγRIIIa (CD32A), on neutrophils and monocytes, leading to cell activation and for ANCA binding to FcγRIIIb (CD16B) (13–16). Syk is essential for FcγRIIIa signaling, suggesting that it may have a role in ANCA-mediated activation of neutrophils and monocytes (3,17). It has previously been demonstrated that activation of neutrophils by ANCA results in phosphorylation of Syk and that this likely involves both FcγRIIIa and FcγRIIIb (18).

We have previously shown that a small molecule kinase inhibitor with selectivity for Syk is an effective treatment for experimental models of vasculitis, although clinical evidence for Syk activation in AAV is lacking (19–21). In this study, we set out to establish whether Syk activation contributes to disease pathogenesis in humans and to identify if Syk inhibition is a viable therapeutic option for multisystem inflammation in AAV.

## PATIENTS AND METHODS

Detailed methods are provided in the Supplementary Materials, available on the *Arthritis & Rheumatology* website at <https://onlinelibrary.wiley.com/doi/10.1002/art.42321>.

**Study approval.** Human AAV biopsy and surgical tissue samples surplus to clinical need were obtained using the Imperial College Healthcare NHS Trust Tissue Bank (application R10015). Blood samples and plasma exchange fluid were obtained from patients with local ethics committee approval (no. 04/Q0406/25 NHS National Research Ethics Committee London - West London & GTAC).

**Neutrophil and monocyte isolation.** Up to 20 ml of EDTA blood was taken from patients with AAV or healthy controls, and neutrophils and peripheral blood mononuclear cells (PBMCs) were isolated using dextran sedimentation and Percoll (Sigma-Aldrich) double-density gradient. Monocytes were then isolated from the PBMC fraction using immunomagnetic negative selection beads (MACS Pan-monocyte Selection Kit; Miltenyi-Biotec).

**Flow cytometry.** PBMCs were used for cell surface staining with antibodies directed against CD14 (Alexa Fluor 594; BioLegend), CD4 (Alexa Fluor 700; BioLegend), CD3 (BV510; BioLegend), CD19 (BV711; BioLegend), CD56 (BV421; BioLegend), CD8a (Alexa Fluor 488; BioLegend), HLA-DR (BV785; BioLegend), and CD16 (BV605; BioLegend). Neutrophils were used for cell surface staining with anti-CD15 (Alexa Fluor 488). For intracellular staining, cells were then fixed in 2% paraformaldehyde, permeabilized using ice-cold 70% methanol, and stained with antibodies against intracellular total Syk (T-Syk) (PE 4D10.2; BioLegend), phosphorylated Syk (P-Syk) 352 (PercP-eFluor710, n3koku5; eBioscience), and P-Syk 348 (allophycocyanin [APC], moch1ct; eBioscience).

**Isolation of MPO-ANCA IgG and control IgG.** MPO-ANCA IgG was isolated from plasma exchange fluid from patients with AAV, and control IgG from serum from healthy controls, using a protein G Sepharose column. F(ab)<sub>2</sub> fragments were prepared using the Pierce F(ab)<sub>2</sub> preparation kit according to the manufacturer's instructions, followed by dialysis (10K MWCO) to remove Fc fragments. Protein content of IgG preparations was quantified by spectrophotometry at 280 nm.

**Neutrophil and monocyte stimulation.** Cells were primed with 2 ng/ml tumor necrosis factor (TNF; PeproTech) for 15 minutes, then stimulated with 100 μg/ml MPO-ANCA IgG, MPO-ANCA IgG F(ab)<sub>2</sub> fragments, or control IgG for 4 hours. If inhibitor was used, it (or vehicle) was added after TNF for 15 minutes prior to the addition of IgG. Interleukin-8 (IL-8) production in supernatant was analyzed using a commercially available IL-8 DuoSet enzyme-linked immunoassay (R&D Systems).

For reactive oxygen species (ROS) production, cells were primed with 2 ng/ml TNF and stimulated with 100 μg/ml MPO-ANCA IgG or control IgG for 1 hour in the presence of 750 nM CellRox DeepRed reagent. As a positive control, 200 μM tert-butyl hydroperoxide was used. Samples were analyzed using a BD Accuri C6 flow cytometer.

**Whole-blood phagocytosis assay.** Blood was collected into 3.8% sodium citrate for use with pHrodo red *Escherichia coli* bioparticles (ThermoFisher). Whole blood was incubated at 37°C with R406 or vehicle (0.01% DMSO) for 15 minutes followed by incubation with bioparticles for 30 minutes. Samples were incubated on ice as a negative control. Samples were then used for cell surface staining with CD14 (BV421), CD16 (BV605), and CD66b (APC; BioLegend) followed by red blood cell lysis. Samples were analyzed using a BD LSR Fortessa flow cytometer.

**RNA extraction and NanoString analysis.** For analysis of gene expression, cells were primed with 2 ng/ml TNF for

15 minutes, then stimulated with MPO-ANCA IgG for 1 hour. If R406 was used, it (or vehicle, 0.01% DMSO) was added after TNF priming for 15 minutes prior to addition of IgG. Total RNA was extracted from cells lysed in TRI reagent (Sigma-Aldrich) using the Direct-zol RNA Miniprep kit (Zymo Research). Next, 100 ng of RNA per sample was used with the human myeloid cell nCounter code set (NanoString Technologies). Normalization of raw gene expression was performed with nSolver Advanced Analysis Software, and low-expression genes were excluded. Clustering and heatmaps of normalized counts were carried out using the clustvis web tool (22). Data were analyzed by Rosalind (<https://rosalind.onramp.bio/>), with a HyperScale architecture.

**Immunohistochemistry.** Immunohistochemistry (IHC) was performed on formalin-fixed paraffin-embedded (FFPE) tissues. Primary antibodies were T-Syk (diluted 1:500, N-19; Santa Cruz Biotechnology) or P-Syk (diluted 1:25, Tyr525/526; Cell Signaling Technology), followed by a secondary polymeric horseradish peroxidase system (EnVision; Dako) and 3,3-diaminobenzidine to develop. For double-staining, primary antibodies used were MPO (diluted 1:1,000; Dako), CD15 (diluted 1:50, Carb-3; Dako), or CD68 (diluted 1:50, PGM1; Dako). StayGreen AP Plus detection kit (Abcam) was used to develop sections, and slides were counterstained with Mayer's hematoxylin and mounted using Vectamount (Vector Labs).

**RNAscope in situ hybridization (ISH).** Detection of Syk messenger RNA (mRNA) in tissue sections was performed using RNAscope on FFPE sections according to the protocol of the manufacturer (ACDBio). For each sample, slides were incubated with a target probe, with peptidylpropyl isomerase B–positive control probe (to check the integrity of mRNA), or with DapB, a bacterial gene as a negative control. Quantification of Syk mRNA was conducted by an observer blinded with regard to the histologic class of disease, using Image J.

**Statistical analysis.** Statistical analysis was performed using GraphPad Prism 9. Results are expressed as the median and interquartile range, and comparisons between groups were conducted by Mann-Whitney U test or Kruskal-Wallis test with Dunn's multiple comparison test. For linear correlation, Pearson's correlation coefficient was used. NanoString data were analyzed by Rosalind, with a HyperScale architecture. The limma R library was used to calculate fold changes and *P* values and perform optional covariate correction (23).

## RESULTS

**Phosphorylated Syk in neutrophils from patients with active AAV.** Using flow cytometry, we compared levels of T-Syk and P-Syk in neutrophils isolated from

patients with AAV (*n* = 35 with active AAV, *n* = 26 with disease in remission) and healthy controls (*n* = 10) (Supplementary Table 1, <https://onlinelibrary.wiley.com/doi/10.1002/art.42321>). As expected, there was no difference in levels of T-Syk between groups (median fluorescence intensity [MFI] 5,637 for patients with active AAV, 4,000 for patients with disease in remission, and 5,055 for healthy controls) (Figure 1A), but there was increased phosphorylation of Syk at the 348 tyrosine residue (Y<sup>348</sup>) (MFI 4,191 for patients with active AAV, 1,016 for patients with disease in remission, and 1,687 for healthy controls; *P* = 0.0002) (Figure 1B). We confirmed this result in a subset of patients (*n* = 23 with active AAV, *n* = 6 with disease in remission), showing that there was increased phosphorylation of Syk at the 352 tyrosine residue (Y<sup>352</sup>), a second activation site, in patients with active AAV compared to healthy controls, although the difference between patients with active AAV and those with disease in remission was not significant (MFI 4,321 for patients with active AAV, 1,817 for patients with disease in remission, and 1,036 for healthy controls; *P* = 0.008) (Figure 1C). In a group of patients who provided a follow-up sample when in disease remission, there was decreased P-Syk (Y<sup>348</sup>) in 12 of 14 patients (MFI 5,855 for patients with active AAV and 926 for patients with disease in remission; *P* = 0.01) (Figure 1D).

There was no difference in levels of T-Syk or P-Syk (Y<sup>348</sup>) when analyzed by ANCA serotype (Supplementary Figures 2A–C, <https://onlinelibrary.wiley.com/doi/10.1002/art.42321>). Syk phosphorylation at the Y<sup>348</sup> residue seemed to increase with ANCA titer, compatible with ANCA-mediated phosphorylation of Syk in circulating neutrophils in vivo (*r* = 0.4, *P* = 0.01) (Figures 1E and F). Levels of neutrophil P-Syk (Y<sup>348</sup>) did not correlate with C-reactive protein (CRP), serum creatinine, or neutrophil count, suggesting that increased levels of Syk phosphorylation are not due to factors causing an increase in neutrophil count, such as concomitant infection or steroid treatment (Figure 1E).

### Phosphorylation of Syk in neutrophils following in vitro MPO-ANCA stimulation and inhibition of MPO-ANCA-induced neutrophil activation by R406.

Stimulation of TNF-primed neutrophils with MPO-ANCA IgG in vitro resulted in rapid phosphorylation of P-Syk (Y<sup>348</sup>), which was maximal by 30 minutes of stimulation and was decreased by 120 minutes. This was not seen in cells stimulated with healthy control IgG in place of MPO-ANCA IgG (Figures 2A and B).

There was significant IL-8 production by neutrophils following MPO-ANCA IgG stimulation (median IL-8 1,001.0 pg/ml with TNF/MPO-ANCA IgG and 177.4 pg/ml with TNF/control IgG; *P* = 0.0003) (Figure 2C). IL-8 production was reduced when F(ab)<sub>2</sub> MPO-ANCA IgG fragments were used in place of whole MPO-ANCA IgG (median neutrophil IL-8 production 677.1 with TNF/MPO-ANCA IgG and 290.3 pg/ml with TNF/F(ab)<sub>2</sub>)

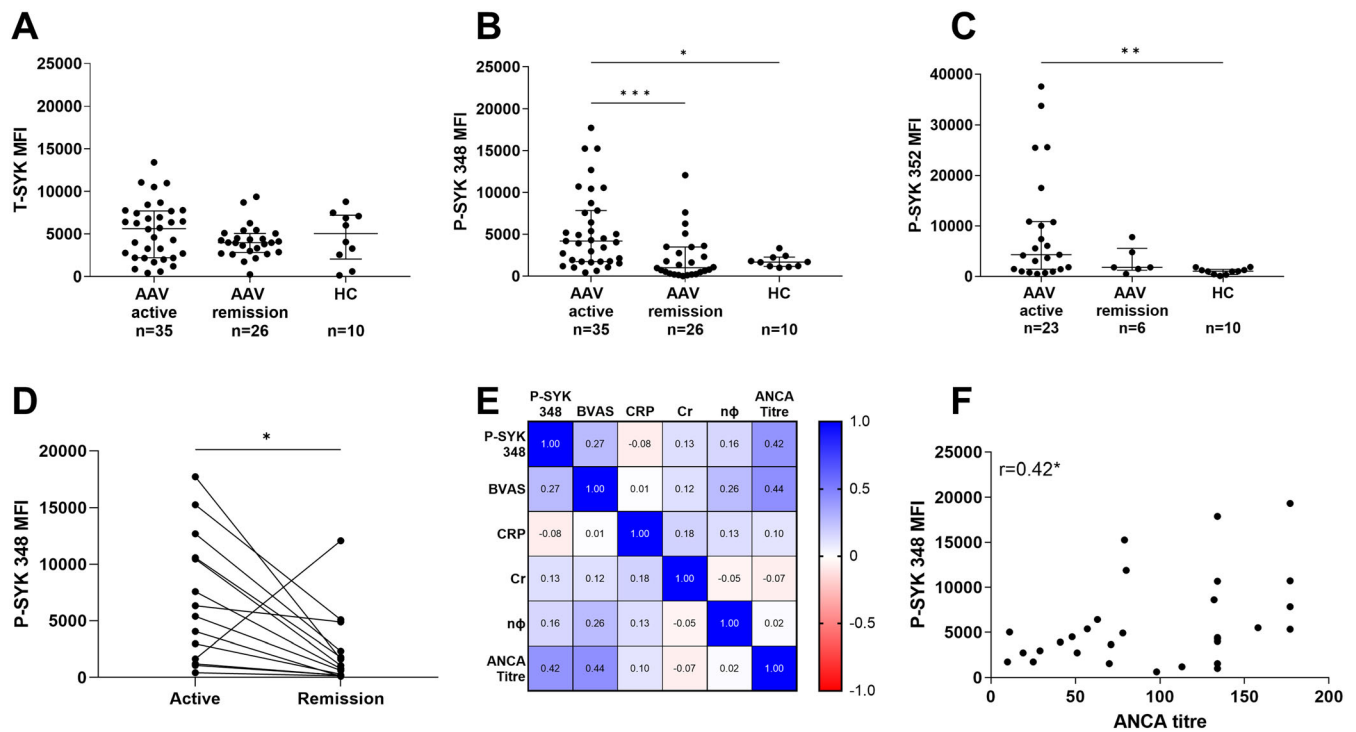


**Figure 1.** Neutrophil Syk is phosphorylated at activation residues in patients with active antineutrophil cytoplasmic antibody (ANCA)-associated vasculitis (AAV). **A–C**, Median fluorescence intensity (MFI) of intracellular total Syk (T-Syk) (**A**), intracellular phosphorylated Syk (P-Syk) at residue Y<sup>348</sup> (**B**), and intracellular P-Syk at residue Y<sup>352</sup> (**C**) in neutrophils isolated from patients with active AAV (n = 35), patients with disease in remission (n = 26), and healthy controls (HC; n = 10). Bars show the median and interquartile range. **D**, Comparison of MFI of intracellular P-Syk (Y<sup>348</sup>) among a subgroup of patients with active AAV (n = 14) who provided a follow-up sample after attaining disease remission. **E**, Correlation matrix of P-Syk (Y<sup>348</sup>) with clinical parameters in patients with active AAV. **F**, Correlation between P-Syk (Y<sup>348</sup>) and ANCA titer in patients with active AAV. Patient characteristics are shown in Supplementary Table 1 (<https://onlinelibrary.wiley.com/doi/10.1002/art.42321>). \* = P < 0.05; \*\* = P < 0.01; \*\*\* = P < 0.001, by Kruskal-Wallis test with Dunn’s post hoc correction (versus the active AAV group) in **A–C**, and by Wilcoxon’s matched pairs signed rank test in **D**. BVAS = Birmingham Vasculitis Activity Score; CRP = C-reactive protein; Cr = serum creatinine; nφ = neutrophil count × 10<sup>9</sup>/ml.

(Figure 2D), suggesting that MPO-ANCA IgG-mediated IL-8 release is partially dependent on FcγR engagement and is consistent with a role for Syk signaling in ANCA-induced neutrophil responses. Moreover, IL-8 release was inhibited in a dose-dependent manner by R406, the active metabolite of fostamatinib, a small molecule inhibitor relatively selective for Syk (median IL-8 685.4 pg/ml with vehicle, 85.7 pg/ml with 2 μM R406, 223.1 pg/ml with 1 μM R406, and 366 pg/ml with 0.2 μM R406; P < 0.0001) (Figure 2C).

In addition to IL-8 release, stimulation of neutrophils with MPO-ANCA IgG resulted in more ROS production compared to cells stimulated with control IgG (median percentage ROS-positive cells 31.0% with MPO-ANCA IgG and 16.1% with control IgG; P = 0.04) (Figures 2E and F). ROS production was also inhibited by R406 (median percentage ROS-positive cells 14.0% with 2 μM R406 and 30.2% with vehicle; P = 0.008) (Figure 2F). At the concentrations used here, R406 is expected to be relatively selective for Syk in vitro (24). In order to confirm that these effects were not due to off-target effects of R406, we used a second Syk inhibitor, entospletinib, to inhibit MPO-ANCA IgG-induced IL-8

and ROS production by neutrophils, demonstrating similar results to R406 (Supplementary Figure 3, <https://onlinelibrary.wiley.com/doi/10.1002/art.42321>). To assess the potential effect of Syk inhibition on non-antibody-mediated functions such as bacterial phagocytosis, which may potentially lead to infection risk in clinical use, we used a whole-blood phagocytosis assay. R406 had no effect on neutrophil phagocytosis of *E coli* bioparticles (Supplementary Figure 4A, <https://onlinelibrary.wiley.com/doi/10.1002/art.42321>).

**Phosphorylation of Syk in monocytes from patients with active AAV and inhibition of MPO-ANCA IgG-induced monocyte responses by R406.**

Monocytes also express the ANCA autoantigens and are increasingly recognized as contributing to the pathogenesis of AAV (25,26). Monocytes express high levels of FcγR1a, suggesting a role for Syk in ANCA IgG-mediated monocyte activation. We therefore assessed Syk activation in monocytes, with the aim of validating our results in neutrophils. Flow cytometry of PBMCs isolated from patients with AAV (n = 12 with active disease, n = 13 with disease in remission)

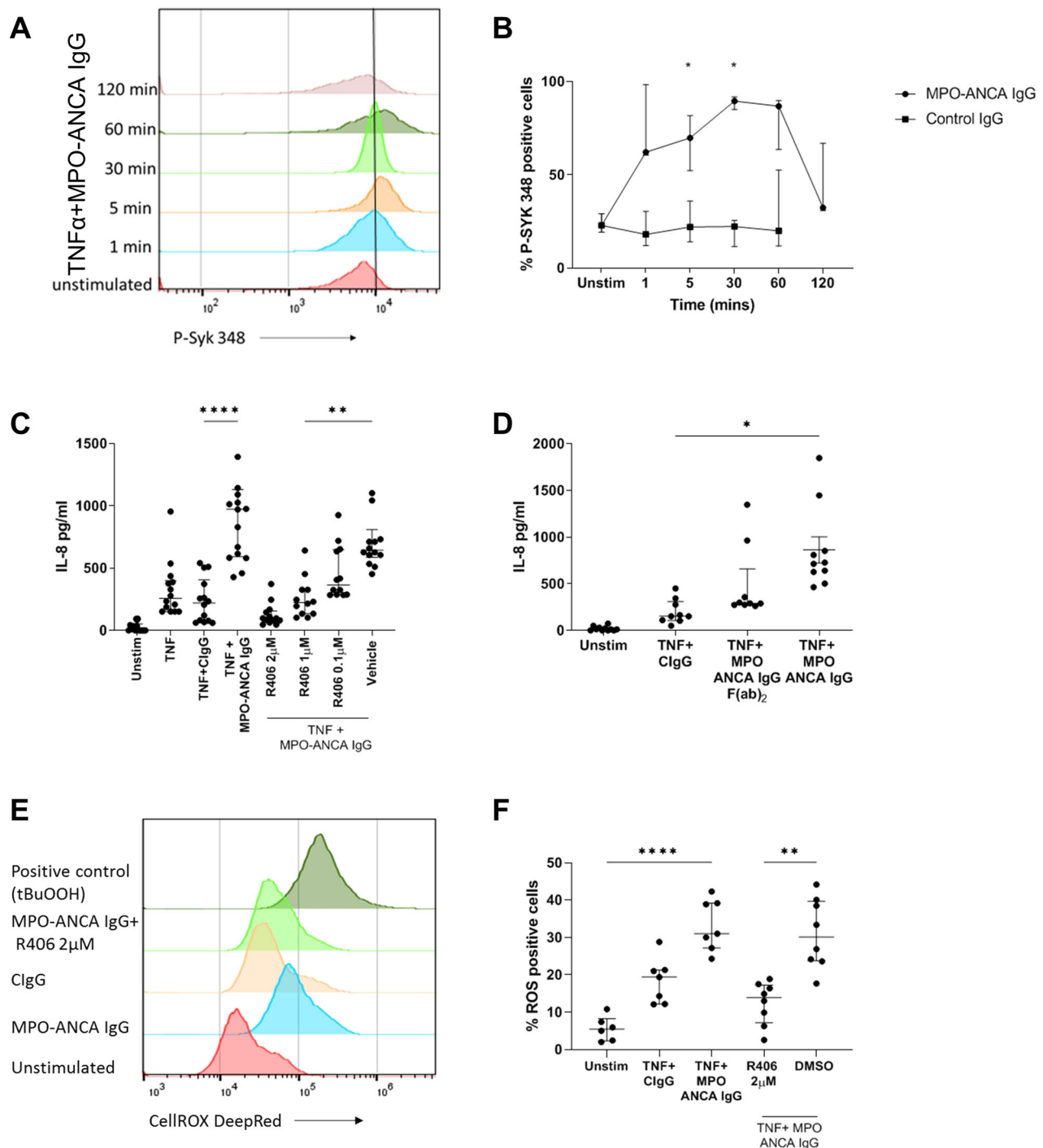


**Figure 2.** Syk is phosphorylated following myeloperoxidase (MPO)–ANCA stimulation, and Syk inhibition can prevent MPO-ANCA–induced responses. **A** and **B**, Representative histogram (**A**) and quantification (**B**) of MFI of P-Syk ( $Y^{348}$ ) in neutrophils isolated from healthy controls and stimulated ex vivo with 2 ng/ml tumor necrosis factor (TNF) for 15 minutes, followed by either 100  $\mu$ g/ml MPO-ANCA IgG or 100  $\mu$ g/ml control IgG (ClgG) for the indicated duration. **C**, Interleukin-8 (IL-8) release from neutrophils isolated from healthy controls primed with 2 ng/ml TNF for 15 minutes and then stimulated with 100  $\mu$ g/ml MPO-ANCA IgG for 4 hours. **D**, IL-8 production from neutrophils isolated from healthy controls and primed with 2 ng/ml TNF for 15 minutes and then stimulated with 100  $\mu$ g/ml MPO-ANCA IgG or F(ab)<sub>2</sub> fragments of 100  $\mu$ g/ml MPO-ANCA IgG for 4 hours. **E** and **F**, Representative histogram (**E**) and quantification (**F**) of reactive oxygen species (ROS) production, by percentage of cells positive for CellRox Deep Red reagent (gated on unstained cells). Cells were primed with 2 ng/ml TNF for 15 minutes and then stimulated with 100  $\mu$ g/ml MPO-ANCA IgG for 1 hour. In **C** and **F**, when R406 or vehicle (0.01% DMSO) were used, they were added to cells for 15 minutes following TNF priming and prior to stimulation with MPO-ANCA IgG. Cells were isolated from  $\geq 3$  healthy donors with  $\geq 2$  biologic replicates for each donor. Bars show the median and interquartile range. \* =  $P < 0.05$ ; \*\* =  $P < 0.01$ ; \*\*\* =  $P < 0.001$ , by Kruskal-Wallis test with Dunn's post hoc correction. Unstim = unstimulated; tBuOOH = *tert*-butyl hydroperoxide (see Figure 1 for other definitions). Color figure can be viewed in the online issue, which is available at <http://onlinelibrary.wiley.com/doi/10.1002/art.42321/abstract>.

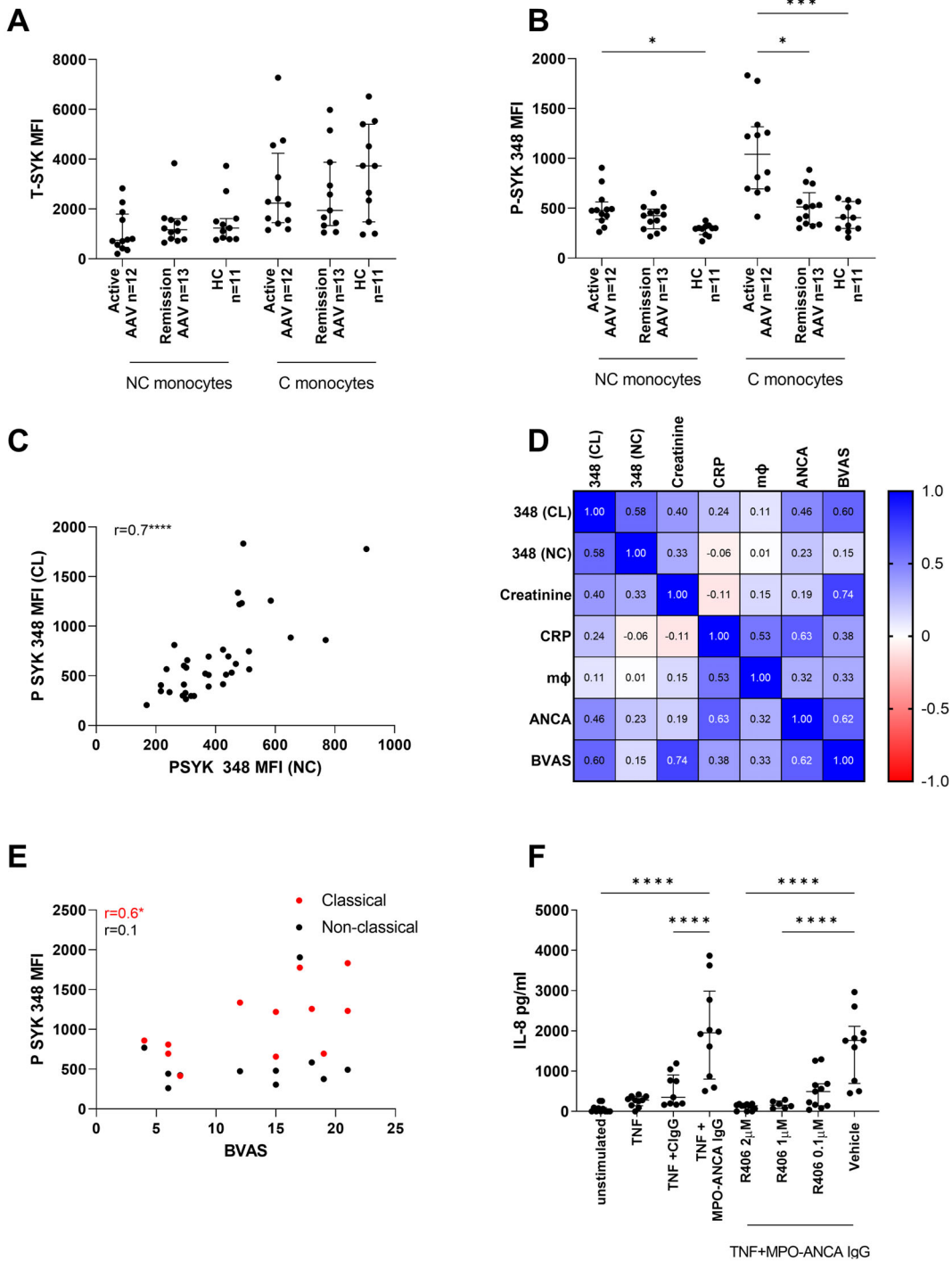


**Figure 3.** Monocyte Syk is phosphorylated at activation residues in patients with active AAV, and monocyte interleukin-8 (IL-8) production in response to myeloperoxidase (MPO)-ANCA IgG can be inhibited by R406. **A** and **B**, MFI of intracellular T-Syk (**A**) and intracellular P-Syk ( $Y^{348}$ ) (**B**) in classical (C) and nonclassical (NC) monocytes isolated from patients with active AAV (n = 12), those with disease in remission (n = 13), and healthy controls (n = 11). P-Syk ( $Y^{348}$ ) is up-regulated in patients with active AAV compared to those with AAV in remission or healthy controls, with a greater magnitude of increase in classical compared to nonclassical monocytes. **C**, Correlation between levels of P-Syk ( $Y^{348}$ ) in classical (CL) and nonclassical (NC) monocytes among the whole cohort. **D**, Correlation matrix of P-Syk ( $Y^{348}$ ) and clinical parameters in patients with active AAV. **E**, Correlation between P-Syk ( $Y^{348}$ ) and BVAS in classical and nonclassical monocytes. **F**, IL-8 production from monocytes primed with 2 ng/ml tumor necrosis factor (TNF) for 15 minutes and then stimulated with 100  $\mu$ g/ml IgG MPO-ANCA for 4 hours. When R406 or vehicle (0.01% DMSO) were used, they were added to cells for 15 minutes following TNF priming and prior to stimulation with MPO-ANCA IgG. Results are from 4 biologic replicate experiments with monocytes isolated from 4 healthy donors. Bars show the median and interquartile range. Gating strategy for monocytes is shown in Supplementary Table 1 (<https://onlinelibrary.wiley.com/doi/10.1002/art.42321>). \* =  $P < 0.05$ ; \*\*\* =  $P < 0.001$ ; \*\*\*\* =  $P < 0.0001$ , by Kruskal-Wallis test with Dunn's post hoc correction. M $\phi$  = monocyte count  $\times 10^9$ /ml (see Figure 1 for other definitions). Color figure can be viewed in the online issue, which is available at <http://onlinelibrary.wiley.com/doi/10.1002/art.42321/abstract>.

and healthy controls ( $n = 11$ ) was performed to assess levels of T-Syk and P-Syk 348 (Supplementary Table 2, <https://onlinelibrary.wiley.com/doi/10.1002/art.42321>). As expected, there was no difference in levels of monocyte T-Syk between the groups, but T-Syk was increased in classical monocytes (CD14++CD16-) compared to nonclassical monocytes (CD14 + CD16++) in all participants (Figure 3A), which is consistent with previous reports of increased Syk gene expression in classical and nonclassical monocytes (27).

P-Syk ( $Y^{348}$ ) was elevated in both classical and nonclassical monocytes in patients with active AAV compared to healthy controls and in classical monocytes in patients with active disease compared to those with disease in remission. Higher levels of Syk phosphorylation were seen in classical versus nonclassical monocytes, in keeping with greater total Syk expression in this cell type (Figure 3B). For the whole cohort (patients and healthy controls), there was strong correlation between P-Syk ( $Y^{348}$ ) in classical and nonclassical monocytes ( $r = 0.7$ ,  $P < 0.0001$ ; Figure 3C). There was no difference in P-Syk ( $Y^{348}$ ) based on ANCA serotype in either monocyte subset, nor were there correlations with CRP, serum creatinine, or total monocyte count (Figure 3D). For classical monocytes, there was weak correlation between levels of P-Syk ( $Y^{348}$ ) and ANCA titers ( $r = 0.459$ ,  $P = 0.1$ ), which was again compatible with ANCA-mediated phosphorylation of Syk in vivo, and there was a moderate correlation between levels of P-Syk ( $Y^{348}$ ) and Birmingham Vasculitis Activity Score (BVAS) ( $r = 0.6$ ,  $P = 0.04$ ; Figure 3E). Levels of T-Syk and P-Syk ( $Y^{348}$ ) in other components of the PBMC fraction, including B cell and natural killer cells, are shown in the Supplementary Figure 5 (<https://onlinelibrary.wiley.com/doi/10.1002/art.42321>).

Consistent with our findings in neutrophils, monocyte IL-8 production following MPO-ANCA IgG stimulation in vitro was Syk-dependent. There was significant IL-8 production in response to MPO-ANCA IgG stimulation compared to control IgG stimulation (median IL-8 1,924 pg/ml with TNF/MPO-ANCA IgG and 752 pg/ml with TNF/control IgG;  $P = 0.02$ ) (Figure 3F), which could be inhibited by R406 in a dose-dependent manner (median IL-8 1,758 pg/ml with vehicle, 138.6 pg/ml with 2  $\mu$ M R406, 155.6 pg/ml with 1  $\mu$ M R406, and 492.9 pg/ml with 0.2  $\mu$ M R406;  $P < 0.0001$ ) (Figure 3F). Similar to our findings with neutrophils, R406 had no effect on monocyte phagocytosis of *E coli* bioparticles (Supplementary Figure 4B, <https://onlinelibrary.wiley.com/doi/10.1002/art.42321>). As expected, there was more phagocytosis mediated by classical compared to nonclassical monocytes.

**Altered myeloid cell gene expression by MPO-ANCA IgG stimulation.** To determine if Syk-dependent signaling pathways are activated in AAV, we next investigated transcriptional differences in MPO-ANCA IgG-stimulated granulocytes and monocytes, and the effect of Syk inhibition with R406 on

these changes, using the NanoString analysis platform. The myeloid innate immunity gene panel used for this study includes 770 genes, covering a range of pathways and processes, including cytokines, chemokines, cell migration and adhesion, and FcR signaling (Figure 4A, Supplementary Figure 6, and Supplementary Table 3, <https://onlinelibrary.wiley.com/doi/10.1002/art.42321>). Compared to unstimulated granulocytes, MPO-ANCA IgG-stimulated granulocytes showed up-regulation of genes in several functional categories, including chemokine and cytokine signaling (*CXCL8*, *CCL20*, *CCL3*, *CC3L1*, *CXCL2*, *CCL4*, *CCRL2*, *IL1A*, *IL1B*, *TNF*, *TRAF1*, *NFKB*, *EDN1*), chemotaxis (*CCL20*, *CCL3*, *CCL4*, *CCL3L1*, *CXCL8*, *IL1B*, *EDN1*, *LGALS3*), and stress response (*NRFA2*, *GADD45A*).

Reflecting their greater plasticity as a non-terminally differentiated cell, monocytes showed a greater degree of transcriptional activity following stimulation with MPO-ANCA IgG, and NanoString analysis identified substantially more differentially expressed genes than observed in neutrophils (Supplementary Figures 7 and 8A and Supplementary Table 4, <https://onlinelibrary.wiley.com/doi/10.1002/art.42321>). The differentially expressed genes in MPO-ANCA IgG-stimulated monocytes included those involved in multiple effector functions, such as the following: 1) genes for proinflammatory chemokines and cytokines, and genes downstream of cytokine receptors such as JAK/STAT and MAPK (Figure 4B and Supplementary Figure 8B); 2) genes involved in cell migration and adhesion (Figure 4C); 3) FcR-dependent pathways (Figure 4D); and 4) genes implicated in the breakdown of extracellular matrix (ECM) (Supplementary Figure 8C). In keeping with a role for Syk in MPO-ANCA IgG-mediated monocyte activation, genes related to tyrosine kinase phosphorylation were also up-regulated (Supplementary Figure 8D, <https://onlinelibrary.wiley.com/doi/10.1002/art.42321>). Specifically, there was up-regulation of genes involved in several Syk-dependent signaling pathways, including those related to positive regulation of Rho GTPase activity. Rho-dependent GTPases have been identified to play a role downstream of Fc $\gamma$ R activation, signaling via Syk, PLC $\gamma$ 2, Vav (also up-regulated), and phosphatidylinositol 3-kinase leading to phagocytosis, ROS, and cytokine production in neutrophils and monocytes (7,28) (Supplementary Figure 8D).

When MPO-ANCA IgG-stimulated cells were pretreated with R406 (and compared to vehicle-treated cells), there was significant down-regulation of the gene signatures, which were found to be up-regulated following MPO-ANCA IgG stimulation in both neutrophils and monocytes (Figures 4E and F and Supplementary Tables 3 and 4, <https://onlinelibrary.wiley.com/doi/10.1002/art.42321>), including those involved in chemokine/cytokine signaling (*CXCL8*, *CCL20*, *CCL3*, *CCL3L1*, *CCL4*, *CCRL2*, *CXCR4*, *CCR1*) (Figure S8E). Similar to the analysis of ANCA-stimulated cells, there was greater transcriptional plasticity of monocytes and treatment with R406 resulted in down-regulation of many genes induced by ANCA IgG stimulation compared to vehicle

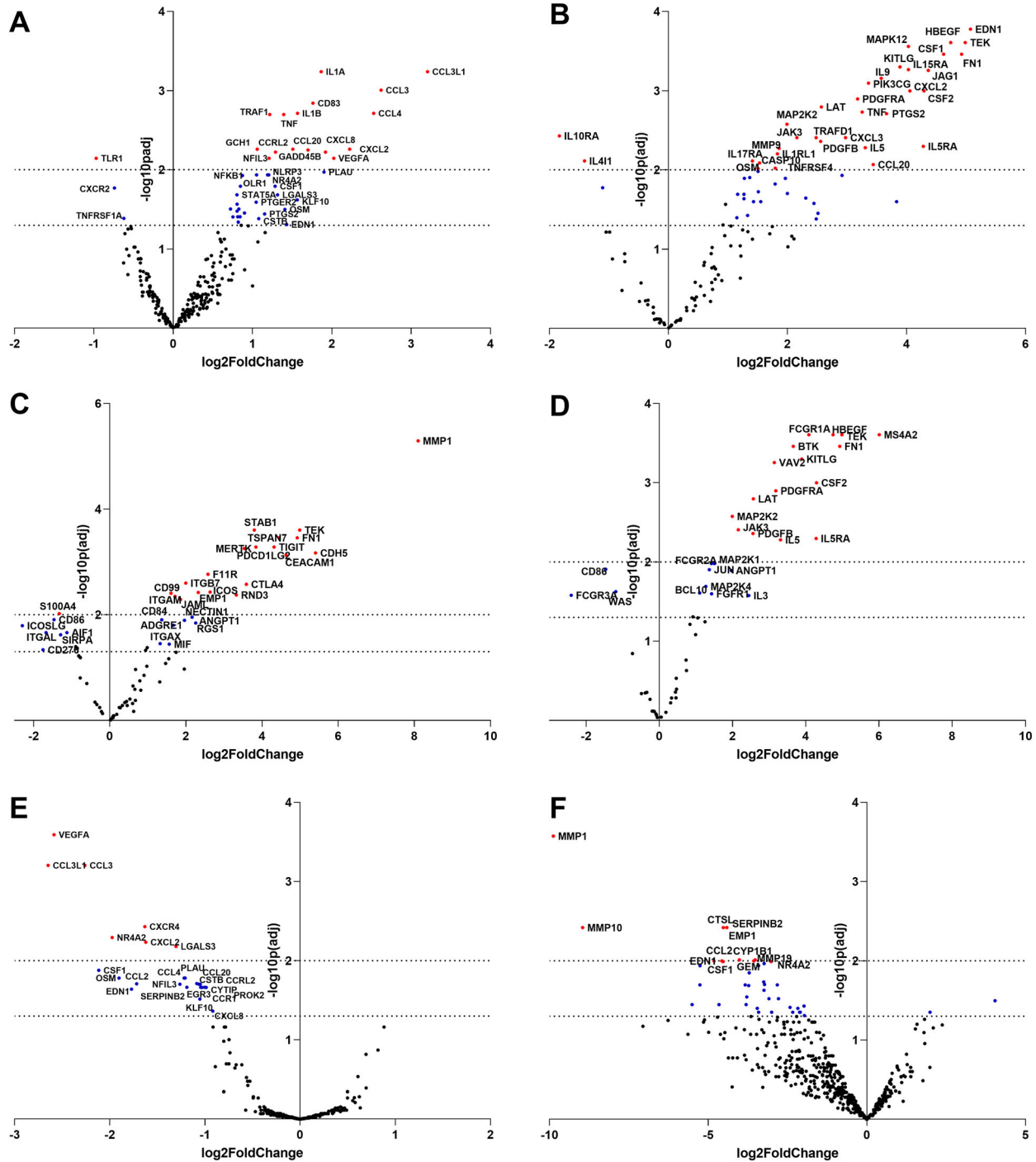


**Figure 4.** NanoString analysis of myeloperoxidase (MPO)–antineutrophil cytoplasmic antibody (ANCA) IgG–stimulated granulocytes and monocytes. **A**, Volcano plot showing  $-\log_{10}(P)$  value and  $\log_2$  (fold change) for granulocytes primed with 2 ng/ml tumor necrosis factor (TNF) for 15 minutes and then stimulated with 100  $\mu\text{g/ml}$  MPO-ANCA IgG for 1 hour, compared to unstimulated granulocytes. All genes included in NanoString analysis are shown. **B–D**, Volcano plots showing  $-\log_{10}(P)$  value and  $\log_2$  (fold change) for monocytes primed with 2 ng/ml TNF for 15 minutes then stimulated with 100  $\mu\text{g/ml}$  MPO-ANCA IgG for 1 hour, compared to unstimulated monocytes. Genes shown are identified in the NanoString code set as involved in cytokine pathways (**B**), cell migration and adhesion (**C**), or Fc receptor signaling (**D**). **E**, Volcano plot showing  $-\log_{10}(P)$  value and  $\log_2$  (fold change) for TNF-primed, MPO-ANCA IgG–stimulated granulocytes pretreated with 2  $\mu\text{M}$  R406, compared to those pretreated with vehicle, for all genes included in NanoString analysis. **F**, Volcano plot showing  $-\log_{10}(P)$  value and  $\log_2$  (fold change) for TNF-primed, MPO-ANCA IgG–stimulated monocytes pretreated with 2  $\mu\text{M}$  R406, compared to those pretreated with vehicle, for all genes included in NanoString analysis. Selected differentially expressed genes with a  $\log_2$  (fold change)  $> 1.5$  and adjusted  $P$  values  $< 0.05$  are identified by name and are shown in red (adjusted  $P < 0.01$ ) and blue (adjusted  $P < 0.05$ ). Color figure can be viewed in the online issue, which is available at <http://onlinelibrary.wiley.com/doi/10.1002/art.42321/abstract>.



treatment, including genes involved in chemokine and cytokine pathways, ECM remodeling, and cell migration and adhesion (Figure 4F, Supplementary Figures 8E and F, and Supplementary Table 4). Genes that are associated with GTPase activity, tyrosine phosphorylation cascades, and MAPK signaling pathways were also down-regulated.

**Up-regulation of Syk mRNA in renal biopsy tissue from patients with active AAV.** Using IHC, we have previously shown that Syk is expressed in the inflamed glomeruli of patients with ANCA-associated glomerulonephritis (AAGN) and that this correlates with Berden disease class (29,30). We sought to validate these findings using RNAscope, a method of in situ hybridization used to detect Syk mRNA that overcomes the potential for nonspecific antibody-binding in standard IHC. We confirmed Syk mRNA expression in the glomeruli of patients with crescentic AAGN, with expression localized to crescents and segmental areas of inflammation that mirrored findings using IHC (Figures 5A–C). There was minimal Syk mRNA expression in the glomeruli of patients with sclerotic lesions or in nonaffected glomeruli in patients with mixed-class disease (Figures 5D–F). Marked Syk mRNA expression was also seen in areas of tubulointerstitial and periglomerular inflammation in patients with both sclerotic and crescentic glomerular disease (Figures 5E and G). In our previous study, we also detected Syk expression in distal tubular epithelial cells, a common site for nonspecific staining in standard IHC; in the current study, we have confirmed that this accurately represents Syk expression using RNAscope to detect Syk mRNA (Figures 5H and I).

**Syk expression at extrarenal sites of vasculitis.** Syk is expressed at extrarenal sites of inflammation in patients with active AAV. Our previous studies have focused on the role of Syk in renal disease (20,30). However, many patients with AAV may have extensive multisystem disease affecting nonrenal organs (31). We therefore investigated Syk expression in biopsy and surgical tissue samples from a range of extrarenal sites of inflammation using IHC for T-Syk and P-Syk, with colocalization for leukocyte markers.

We first examined tissue with evidence of small vessel vasculitis and capillaritis, including nerve, skin, and intestinal tissue. We detected T-Syk within cells of perivascular infiltrate of the vasa nervorum that colocalized with the ANCA autoantigen MPO (Figures 6A and B and Supplementary Figures 9A and B, <https://onlinelibrary.wiley.com/doi/10.1002/art.42321>). T-Syk was present in cells with typical neutrophil morphology in inflammatory infiltrate in ear, nose, and throat-associated vasculitis (Figure 6C). T-Syk could also be identified in gut tissue in infiltrating leukocytes associated with vasculitis of an arteriole and leukocytoclasia (Figure 6D). T-Syk was expressed in infiltrating cells at sites of capillaritis in the skin and colocalized with both MPO and the neutrophil marker CD15 (Figures 6E–G and Supplementary Figures 9C–E).

Extravascular granulomatous tissue inflammation is also a common disease manifestation in AAV, and we identified T-Syk in cells within granulomata in lung, nasal, and cutaneous tissue of patients with active AAV affecting these organ sites (Figure 6H and Supplementary Figures 9F–H, <https://onlinelibrary.wiley.com/doi/10.1002/art.42321>). Within areas of severe inflammation in the skin, foamy macrophages were positive for T-Syk, and costaining for CD68 confirmed that T-Syk coexpression was in both monocytes/tissue macrophages and multinucleated giant cells. Importantly, staining for P-Syk was present, indicating Syk activation in these cells in tissue (Figures 6I–K and Supplementary Figures 9I–N). Of note, T-Syk also colocalized with expression of the ANCA autoantigen MPO (Figure 6L and Supplementary Figures 9I–K).

## DISCUSSION

This study identifies a role for Syk in the pathogenesis of AAV and indicates that Syk inhibition may be an effective therapeutic strategy. We showed the up-regulation of Syk phosphorylation (i.e., activation) in circulating innate immune cells in patients with active untreated AAV and found that this correlates with measures of disease activity. We demonstrated that Syk inhibition can prevent ANCA-mediated cellular responses in vitro, including IL-8 and ROS production, and by using targeted gene expression analysis, we confirmed that Syk-dependent signaling pathways were activated following MPO-ANCA IgG stimulation. Finally, we identified Syk in tissue leukocytes at sites of organ inflammation in AAV, using both standard protein IHC and in situ hybridization for Syk mRNA.

In the first component of this study, we examined circulating neutrophils and monocytes from patients with acute AAV, isolated before receipt of immunosuppression, thus providing a unique opportunity to assess the association of Syk expression and activation in myeloid cells with disease activity. The increased phosphorylation of Syk in patients with active untreated AAV and the positive correlation with ANCA titers suggest that ANCA-mediated phosphorylation of myeloid cells may be occurring in vivo and that Syk activation has a role in disease pathogenesis. The tyrosine residue for which we identified the greatest difference in phosphorylation between patients with active disease and those in remission or healthy donors was Y<sup>348</sup>. This residue has been shown to play a critical role in the transition of Syk from an autoinhibited to an activated state (10). The differences in Y<sup>352</sup> phosphorylation were less marked. The reasons for this are likely to be multifactorial and may include technical differences between the 2 antibodies used, differences in kinetics of phosphorylation, or basal phosphorylation states between the 2 sites. A reduction in myeloid cell Syk activation in most patients during clinical remission also suggests a functional correlation with disease activity, although a direct effect of immunosuppressive treatment cannot be

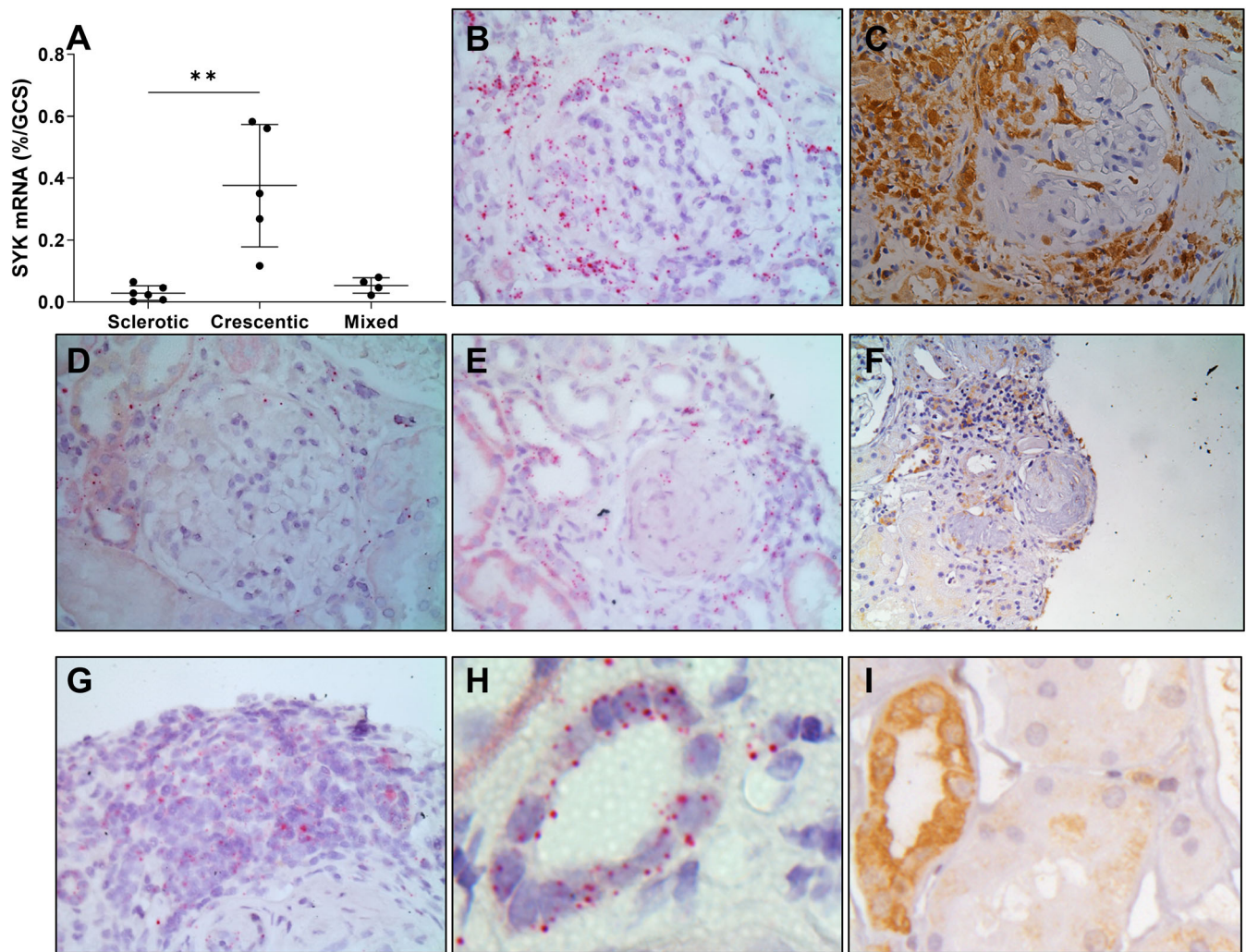


**Figure 5.** Syk mRNA is up-regulated in glomeruli of patients with crescentic antineutrophil cytoplasmic antibody-associated vasculitis. **A**, Quantification of glomerular expression of Syk mRNA using RNAscope in situ hybridization showing significant up-regulation in glomeruli from patients with crescentic glomerulonephritis compared to those with sclerotic (inactive) disease. Bars show the median and interquartile range.  $** = P < 0.01$  by Kruskal-Wallis test with Dunn's post-test comparison. **B**, Representative histologic sections showing Syk mRNA in the distribution of a cellular crescent, likely indicating Syk in infiltrating leukocytes. **C**, Comparative image of immunohistochemistry (IHC) for total Syk (T-Syk) showing positive cells in the distribution of a cellular crescent and periglomerular infiltrate. **D**, Syk mRNA absent in a glomerulus containing a sclerotic lesion. **E**, A small amount of Syk mRNA in a sclerotic glomerulus with significant periglomerular inflammation containing Syk-positive cells. **F**, Comparative image of T-Syk IHC showing negative glomerular staining in a patient with sclerotic disease and T-Syk-positive cells in periglomerular infiltrate. **G**, Syk mRNA in cells in tubulointerstitial infiltrate. **H**, Syk mRNA in cells with characteristic morphology of distal tubular epithelial cells. **I**, Comparative image of T-Syk IHC showing positive staining of distal tubular epithelial cells. In **B–I**, original magnification  $\times 400$  with hematoxylin counterstain. IHC images show immunoperoxidase staining. Color figure can be viewed in the online issue, which is available at <http://onlinelibrary.wiley.com/doi/10.1002/art.42321/abstract>.

excluded. In acute disease, a range of Syk activation was observed, suggesting that flow cytometry cell phenotyping could be used to stratify patients for future clinical studies, in order to identify those likely to benefit from Syk inhibitor treatment.

Using the same flow cytometric approach for intracellular phosphoprotein analysis, we next assessed Syk activation in neutrophil responses *in vitro*. It is already established that Syk is activated following Fc $\gamma$ R ligation on neutrophils and monocytes, such

as following immune complex stimulation (32). The active metabolite of fostamatinib, R406 (a small molecule kinase inhibitor with relative selectivity for Syk), can prevent respiratory burst and cytokine release induced by this pathway (1,24,32,33). The role of Fc $\gamma$ R signaling via Syk in ANCA-mediated cell activation is less clearly defined. Several studies have shown the importance of ANCA binding to Fc $\gamma$ R1a in proinflammatory neutrophil responses and that blockade of this receptor decreases ANCA-induced neutrophil activation (13,16). However, studies using F(ab) fragments

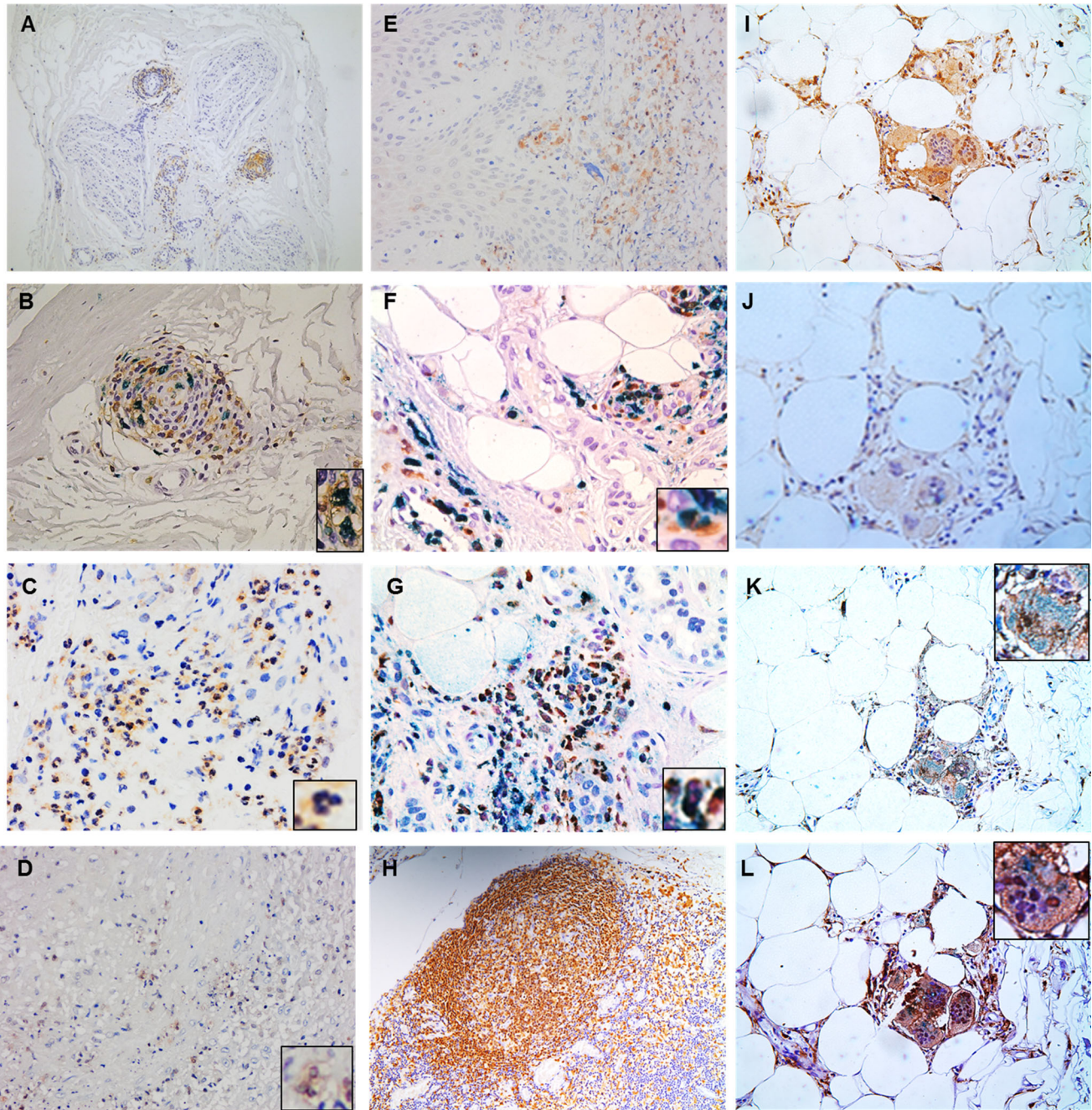


**Figure 6.** Syk is expressed at extrarenal sites of inflammation in patients with active AAV and colocalizes with CD68, CD15, and myeloperoxidase (MPO). Immunohistochemistry for Syk on biopsy tissue from extrarenal sites of inflammation in patients with AAV was performed. **A** and **B**, Low-power image of perivascular infiltrate of the vasa nervorum showing cells positive for T-Syk (brown) (**A**) and high-power image showing cells positive for T-Syk (brown) and MPO (blue), with cells positive for MPO and T-Syk magnified (**inset**) (**B**). **C**, Paranasal sinus tissue showing infiltrate of Syk-positive neutrophils and mononuclear cells, including those with typical neutrophil nuclear morphology (**inset**). **D**, Vasculitis of an arteriole in the gut with evidence of leukocytoclasia, with T-Syk-positive cells magnified (**inset**). **E–G**, Low-power image of capillaritis in cutaneous tissue with evidence of leukocytoclasia showing cells positive for T-Syk (brown) (**E**) and high-power images showing T-Syk (brown) and CD15 (blue) (**F**) and T-Syk (brown) and MPO (blue) (**G**). **Insets** show magnified images of cells positive for T-Syk and CD15 or MPO, respectively. **H**, Inflammation in the lung showing dense collection of T-Syk-positive cells. **I–L**, An area of severe inflammation in the skin with foamy macrophages positive for T-Syk (**I**), P-Syk (**J**), T-Syk (brown) and CD68 (blue) (**K**), and T-Syk (brown) and MPO (blue) (**L**). **Insets** show magnified images of cells positive for T-Syk and CD68 or MPO, respectively. Immunoperoxidase/immunophosphatase staining is shown with hematoxylin counterstain. Original magnification  $\times 100$  (**A** and **E**),  $\times 200$  (**D**, **H–L**),  $\times 400$  (**B**, **C**, **F**, **G**). Single stains and additional images are shown in Supplementary Figure 9 (<https://onlinelibrary.wiley.com/doi/10.1002/art.42321>). See Figure 1 for other definitions.

of ANCA IgG have generated conflicting results. Several have shown that F(ab) fragments can bind neutrophils but that this does not result in cell activation. Others have shown that cross-linked F(ab) or F(ab)<sub>2</sub> of ANCA can induce neutrophil activation, resulting in cytokine release and the production of ROS, although this is not a consistent finding (15,34–36). Our findings identify a critical role for Syk in mediating MPO-ANCA IgG responses, suggesting that FcγR-dependent signaling is necessary for ANCA-induced activation of myeloid cells. Consistent with this finding, we showed that stimulation with F(ab)<sub>2</sub> fragments in place of whole IgG results in decreased but not abolished cytokine release. It is likely that several mechanisms lead to ANCA-induced activation of myeloid cells in AAV, requiring binding to both auto-antigen and FcR, such as in the Kurlander effect (37).

Transcriptional analysis of both granulocytes and monocytes after stimulation with MPO-ANCA IgG identified up-regulation of several pathways likely to contribute to disease pathogenesis in AAV, including chemokine/cytokine production and chemotaxis in neutrophils. Monocytes, having greater plasticity, showed broader changes in transcriptional activity, involving genes related to cytokine/chemokine production and response, genes implicated in the breakdown of extracellular matrix, and genes involved in cell migration and adhesion. Notably, there was clear differential expression of genes involved in FcR signaling, including significant up-regulation of Rho GTPases, and of genes known to increase their activity. In cells treated with R406, these pathways were down-regulated to levels seen in unstimulated cells. Several studies have identified a role for these proteins downstream of FcγR/Syk signaling, and we suggest that activation of Syk and downstream signaling through PLCγ/Vav/Ras/MAPK/NF-κB leads to myeloid cell activation and cytokine production after stimulation with MPO-ANCA IgG (38,39).

Having identified increased Syk activation in circulating innate immune cells of patients with acute AAV and a role for Syk signaling in MPO-ANCA IgG-mediated activation of myeloid cells *in vitro*, we next sought to investigate Syk expression and activation in the tissue of organs affected by vasculitis. Using RNAscope ISH, we confirm the specificity of our previous studies using standard IHC and identify that glomerular Syk mRNA expression is highest in those with crescentic glomerulonephritis and lowest in those with sclerotic (i.e., histologically inactive) disease (30). Syk expression within glomeruli was localized to areas of crescent formation or segmental proliferation and was also observed in areas of tubulointerstitial and periglomerular inflammation. We used this standard IHC approach to show that Syk is expressed and phosphorylated at multiple sites of extrarenal organ inflammation in AAV, including in the lungs and the upper respiratory tract, skin, nerve, and intestinal tissue. These results suggest that inhibition of Syk may have broad therapeutic potential for the diverse clinical

manifestations of AAV, including extravascular granulomatous tissue inflammation.

Our study has some limitations. Not all patients provided sequential samples for analysis, and so we were unable to investigate changes in Syk activation prior to relapse, nor could we exclude a direct effect of immunosuppression on Syk activation in the remission group. It was also not possible to quantify Syk activation in tissue due to the technical limitations of IHC, a non-stoichiometric technique. However, our findings suggest a role for Syk in the pathogenesis of AAV and that drugs targeting Syk may provide a novel treatment approach in this disease. Fostamatinib, the orally administered prodrug form of R406, is now an established therapeutic (40,41). In immune thrombocytopenia, this therapy has shown efficacy in refractory disease and an acceptable toxicity profile (41). Despite its effects on inhibiting myeloid cell activation, fostamatinib/R406 does not seem to increase the risk of bacterial infection, and the most commonly reported side effects in clinical studies were gastrointestinal disturbance and mild hypertension (3–5-mmHg increase in systolic blood pressure), which can usually be managed without cessation of the drug. In biochemical kinase assays, R406 has been shown to have activity at a number of other kinases with similar or greater potency than it has for Syk, although in cell-based assays, this was reduced when compared to its activity at Syk (24,42,43). R406 has also been shown to have activity at vascular endothelial growth factor receptor 2, which is likely to explain its small effect on blood pressure in clinical studies (43). However, this pathway is unlikely to mediate the effect seen on ANCA-mediated myeloid cell activation *in vitro*, and inhibition of Syk, downstream of FcR, is the most biologically plausible explanation. As there is the possibility that R406 may be acting at other targets than Syk *in vitro*, we have confirmed our results in neutrophils, using a second inhibitor entospletinib, which is described to be selective for Syk.

This study focused on Syk expression and activation in innate immune cells, although it is recognized that B cell maturation, survival, and activation are Syk-dependent (44). B cell-directed therapy is an established strategy in the treatment of AAV, and disruption of these Syk-dependent B cell functions with fostamatinib treatment may provide additional therapeutic benefit (45). Of interest, we found evidence of Syk activation in B cells from patients with active disease (Supplementary Figure 5, <https://onlinelibrary.wiley.com/doi/10.1002/art.42321>), and the role of Syk in humoral immunity in AAV should be explored in future studies.

We have previously shown that fostamatinib is an effective treatment for pulmonary and renal disease in preclinical models of vasculitis, and, based on our findings here that show convincing evidence of Syk activation in patients with AAV, we suggest that Syk inhibition with fostamatinib should be prioritized for future clinical studies in vasculitis (21,46).

## ACKNOWLEDGMENTS

Human tissue samples used in this research project were obtained from the Imperial College Healthcare Tissue Bank (ICHTB). ICHTB is supported by the NIHR Biomedical Research Centre based at Imperial College Healthcare NHS Trust and Imperial College London.

## AUTHOR CONTRIBUTIONS

All authors were involved in drafting the article or revising it critically for important intellectual content, and all authors approved the final version to be published. Dr. Prendecki had full access to all of the data in the study and takes responsibility for the integrity of the data and the accuracy of the data analysis.

**Study conception and design.** Prendecki, Pusey, McAdoo.

**Acquisition of data.** Prendecki, Gulati, Pisacano, Pinheiro, Bhatt, Mawhin, Toulza, Cowburn, Lodge.

**Analysis and interpretation of data.** Prendecki, Masuda, Tam, Roufosse, Pusey, McAdoo.

## REFERENCES

- Mocsai A, Ruland J, Tybulewicz VL. The Syk tyrosine kinase: a crucial player in diverse biological functions [review]. *Nat Rev Immunol* 2010; 10:387–402.
- Crowley MT, Costello PS, Fitzer-Attas CJ, et al. A critical role for Syk in signal transduction and phagocytosis mediated by Fc $\gamma$  receptors on macrophages. *J Exp Med* 1997;186:1027–39.
- Kiefer F, Brumell J, Al-Alawi N, et al. The Syk protein tyrosine kinase is essential for Fc $\gamma$  receptor signaling in macrophages and neutrophils. *Mol Cell Biol* 1998;18:4209–20.
- Geahlen RL. Syk and pTyr<sup>d</sup>: signaling through the B cell antigen receptor [review]. *Biochim Biophys Acta* 2009;1793:1115–27.
- Tsang E, Giannetti AM, Shaw D, et al. Molecular mechanism of the Syk activation switch. *J Biol Chem* 2008;283:32650–9.
- Turner M, Schweighoffer E, Colucci F, et al. Tyrosine kinase Syk: essential functions for immunoreceptor signalling. *Immunol Today* 2000;21:148–54.
- Futosi K, Mócsai A. Tyrosine kinase signaling pathways in neutrophils [review]. *Immunol Rev* 2016;273:121–39.
- Gradler U, Schwarz D, Dresing V, et al. Structural and biophysical characterization of the Syk activation switch. *J Mol Biol* 2013;425:309–33.
- Pelosi M, Di Bartolo V, Mounier V, et al. Tyrosine 319 in the interdomain B of ZAP-70 is a binding site for the Src homology 2 domain of Lck. *J Biol Chem* 1999;274:14229–37.
- Mansueto MS, Reens A, Rakhilina L, et al. A reevaluation of the spleen tyrosine kinase (Syk) activation mechanism. *J Biol Chem* 2019;294:7658–68.
- Falk RJ, Terrell RS, Charles LA, et al. Anti-neutrophil cytoplasmic autoantibodies induce neutrophils to degranulate and produce oxygen radicals in vitro. *Proc Natl Acad Sci U S A* 1990;87:4115–9.
- Savage CO, Gaskin G, Pusey CD, et al. Anti-neutrophil cytoplasmic antibodies can recognize vascular endothelial cell-bound anti-neutrophil cytoplasm antibody-associated autoantigens. *Exp Nephrol* 1993;1:190–5.
- Porges AJ, Redecha PB, Kimberly WT, et al. Anti-neutrophil cytoplasmic antibodies engage and activate human neutrophils via Fc $\gamma$  RIIa. *J Immunol (Baltimore)* 1994;153:1271–80.
- Kocher M, Edberg JC, Fleit HB, et al. Antineutrophil cytoplasmic antibodies preferentially engage Fc $\gamma$  RIIIb on human neutrophils. *J Immunol (Baltimore)* 1998;161:6909–14.
- Weidner S, Neupert W, Goppelt-Strube M, et al. Antineutrophil cytoplasmic antibodies induce human monocytes to produce oxygen radicals in vitro. *Arthritis Rheum* 2001;44:1698–706.
- Mulder AH, Heeringa P, Brouwer E, et al. Activation of granulocytes by anti-neutrophil cytoplasmic antibodies (ANCA): a Fc $\gamma$  RII-dependent process. *Clin Exp Immunol* 1994;98:270–8.
- Chacko GW, Brandt JT, Coggeshall KM, et al. Phosphoinositide 3-kinase and p72syk noncovalently associate with the low affinity Fc $\gamma$  receptor on human platelets through an immunoreceptor tyrosine-based activation motif. Reconstitution with synthetic phosphopeptides. *J Biol Chem* 1996;271:10775–81.
- Hewins P, Williams JM, Wakelam MJ, et al. Activation of Syk in neutrophils by antineutrophil cytoplasm antibodies occurs via Fc $\gamma$  receptors and CD18. *J Am Soc Nephrol* 2004;15:796–808.
- Smith J, McDaid JP, Bhargal G, et al. A spleen tyrosine kinase inhibitor reduces the severity of established glomerulonephritis. *J Am Soc Nephrol* 2010;21:231–6.
- McAdoo SP, Reynolds J, Bhargal G, et al. Spleen tyrosine kinase inhibition attenuates autoantibody production and reverses experimental autoimmune GN. *J Am Soc Nephrol* 2014;25:2291–302.
- McAdoo SP, Prendecki M, Tanna A, et al. Spleen tyrosine kinase inhibition is an effective treatment for established vasculitis in a pre-clinical model. *Kidney Int* 2020;97:1196–207.
- Metsalu T, Vilo J. ClustVis: a web tool for visualizing clustering of multivariate data using Principal Component Analysis and heatmap. *Nucleic Acids Res* 2015;43:W566–70.
- Ritchie ME, Phipson B, Wu D, et al. Limma powers differential expression analyses for RNA-seq and microarray studies. *Nucleic Acids Res* 2015;43:e47.
- Brasemann S, Taylor V, Zhao H, et al. R406, an orally available spleen tyrosine kinase inhibitor blocks Fc receptor signaling and reduces immune complex-mediated inflammation. *J Pharmacol Exp Ther* 2006;319:998.
- Jennette JC, Falk RJ. ANCA-associated vasculitis: a review. *Clin J Am Soc Nephrol* 2015;10:4–6.
- Tarzi RM, Liu J, Schneiter S, et al. CD14 expression is increased on monocytes in patients with anti-neutrophil cytoplasm antibody (ANCA)-associated vasculitis and correlates with the expression of ANCA autoantigens. *Clin Exp Immunol* 2015;181:65–75.
- Wong KL, Tai JJ, Wong WC, et al. Gene expression profiling reveals the defining features of the classical, intermediate, and nonclassical human monocyte subsets. *Blood* 2011;118:e16–31.
- Turner M, Billadeau DD. VAV proteins as signal integrators for multi-subunit immune-recognition receptors [review]. *Nat Rev Immunol* 2002;2:476–86.
- Berden AE, Ferrario F, Hagen EC, et al. Histopathologic classification of ANCA-associated glomerulonephritis. *J Am Soc Nephrol* 2010; 21:1628.
- McAdoo SP, Bhargal G, Page T, et al. Correlation of disease activity in proliferative glomerulonephritis with glomerular spleen tyrosine kinase expression. *Kidney Int* 2015;88:52–60.
- Savage J, Davies D, Falk RJ, et al. Antineutrophil cytoplasmic antibodies and associated diseases: a review of the clinical and laboratory features. *Kidney Int* 2000;57:846–62.
- Kiener PA, Rankin BM, Burkhardt AL, et al. Cross-linking of Fc $\gamma$  receptor I (Fc $\gamma$  RI) and receptor II (Fc $\gamma$  RII) on monocytic cells activates a signal transduction pathway common to both Fc receptors that involves the stimulation of p72 Syk protein tyrosine kinase. *J Biol Chem* 1993;268:24442–8.
- Coxon A, Cullere X, Knight S, et al. Fc $\gamma$  RIII mediates neutrophil recruitment to immune complexes. A mechanism for neutrophil accumulation in immune-mediated inflammation. *Immunity* 2001;14:693–704.

34. Kettritz R, Jennette JC, Falk RJ. Crosslinking of ANCA-antigens stimulates superoxide release by human neutrophils. *J Am Soc Nephrol* 1997;8:386–94.
35. Ralston DR, Marsh CB, Lowe MP, et al. Antineutrophil cytoplasmic antibodies induce monocyte IL-8 release. Role of surface proteinase-3,  $\alpha$ 1-antitrypsin, and Fc $\gamma$  receptors. *J Clin Invest* 1997;100:1416–24.
36. Cockwell P, Brooks CJ, Adu D, et al. Interleukin-8: a pathogenetic role in antineutrophil cytoplasmic autoantibody-associated glomerulonephritis. *Kidney Int* 1999;55:852–63.
37. Kurlander RJ. Blockade of Fc receptor-mediated binding to U-937 cells by murine monoclonal antibodies directed against a variety of surface antigens. *J Immunol (Baltimore)* 1983;131:140–7.
38. Jakus Z, Simon E, Frommhold D, et al. Critical role of phospholipase C $\gamma$ 2 in integrin and Fc receptor-mediated neutrophil functions and the effector phase of autoimmune arthritis. *J Exp Med* 2009;206:577–93.
39. Cremasco V, Graham DB, Novack DV, et al. Vav/Phospholipase C $\gamma$ 2-mediated control of a neutrophil-dependent murine model of rheumatoid arthritis. *Arthritis Rheum* 2008;58:2712–22.
40. Weinblatt ME, Kavanaugh A, Genovese MC, et al. An oral spleen tyrosine kinase (Syk) inhibitor for rheumatoid arthritis. *New Engl J Med* 2010;363:1303–12.
41. Bussel J, Arnold DM, Grossbard E, et al. Fostamatinib for the treatment of adult persistent and chronic immune thrombocytopenia: results of two phase 3, randomized, placebo-controlled trials. *Am J Hematol* 2018;93:921–30.
42. Davis MI, Hunt JP, Herrgard S, et al. Comprehensive analysis of kinase inhibitor selectivity. *Nat Biotech* 2011;29:1046–51.
43. Rolf MG, Curwen JO, Veldman-Jones M, et al. In vitro pharmacological profiling of R406 identifies molecular targets underlying the clinical effects of fostamatinib. *Pharmacol Res Perspect* 2015;3:e00175.
44. Schweighoffer E, Vanes L, Nys J, et al. The BAFF receptor transduces survival signals by co-opting the B cell receptor signaling pathway. *Immunity* 2013;38:475–88.
45. Jones RB, Tervaert JW, Hauser T, et al. Rituximab versus Cyclophosphamide in ANCA-associated renal vasculitis. *New Engl J Med* 2010;363:211–20.
46. Predecki M, Gulati K, Turner-Stokes T, et al. Characterisation of an enhanced preclinical model of experimental MPO-ANCA autoimmune vasculitis. *J Pathol* 2021;255:107–19.